Bone Reports 18 (2023) 101649

Contents lists available at ScienceDirect

Bone Reports

journal homepage: www.elsevier.com/locate/bonr

Temporomandibular joint arthritis increases canonical Wnt pathway expression in the articular cartilage and trigeminal ganglion in rats

Luane Macêdo de Sousa [a], Ana Carolina de Figueiredo Costa [b], Anamaria Falcão Pereira [c], Conceição da Silva Martins [a], Osias Vieira de Oliveira Filho [b], Paula Goes [a,b], Mariana Lima Vale [a,c], Delane Viana Gondim [a,b,*]

[a] Postgraduate Program in Morphofunctional Sciences, Faculty of Medicine, Federal University of Ceará, Brazil
[b] Postgraduate Program in Dentistry, Faculty of Pharmacy, Dentistry and Nursing, Federal University of Ceará, Brazil
[c] Postgraduate Program in Pharmacology, Faculty of Medicine, Federal University of Ceará, Brazil

ARTICLE INFO

Keywords:
Rheumatoid arthritis
Temporomandibular joint
Wnt signaling pathway
Inflammation
Nociception
Nervous tract markers

ABSTRACT

The canonical Wnt pathway participates in inflammatory diseases and it is involved in neuropathic pain. This study evaluated the immunoexpression of the canonical Wnt signaling pathway in the articular cartilage of the temporomandibular joint (TMJ) and along the nociceptive trigeminal pathway in arthritic rats. For this, male Wistar rats were divided into Control (C) and Arthritic (RA) groups. Arthritis induction was performed through subcutaneous injection of methylated bovine serum albumin (mBSA) and complete Freund Adjuvant (CFA)/ Incomplete Freund Adjuvant (IFA) on the first 14 days (once a week), followed by 3 weekly intra-articular injections of mBSA (10 μl/joint; left TMJ). The following parameters were evaluated: nociceptive threshold, inflammatory infiltrate, type I and III collagen birefringence, immunohistochemistry for IL-1β, TNF-α, IL-6, Wnt10b, β-catenin, cyclin-D1 in articular cartilage, c-Myc in synovial membrane, and immunofluorescence analysis for c-Fos, Wnt-10b and β-catenin in the trigeminal ganglion and the trigeminal subnucleus caudalis. The RA group showed intense articular cartilage damage with proliferation of type III collagen, increased immunoexpression of proinflammatory cytokines and Wnt-10b, β-catenin and cyclin-D1 in the articular cartilage and c-Myc in the synovial membrane. In the RA group, a reduction in the nociceptive threshold was observed, followed by a significant increase in the expression of Wnt-10b in neurons and β-catenin in satellite cells of the trigeminal ganglion. c-Fos immunoexpression was observed in neurons, peripherally and centrally, in arthritic rats. Our data demonstrated that TMJ arthritis in rats causes articular cartilage damage and nociceptive behavior, with increased immunoexpression of canonical Wnt pathway in the articular cartilage and trigeminal ganglion.

1. Introduction

Rheumatoid arthritis (RA) is an inflammatory disease caused by chronic synovial inflammation and destruction of cartilage and bone tissue (Sodhi et al., 2015). It is the most common inflammatory arthritis associated with (temporomandibular joint) TMJ dysfunction (Mustafa et al., 2022). The TMJ RA is underestimated (Covert et al., 2021). and studies relate that 19 % to 85.7 % of patients with RA show TMJ changes, and the symptoms can include joint pain, swelling, limited jaw movement, and even ankylosis (Ruparelia et al., 2014;Ahmed et al., 2015; Kroese et al., 2020; Mustafa et al., 2022).

The canonical Wnt (Wnt/β-catenin) pathway participates in many pathological conditions (Singh et al., 2015; Humphries and Mlodzik, 2018). Several studies associate aberrant Wnt signaling in the development of rheumatic diseases (Baron and Kneissel, 2013; van den Bosch et al., 2017). Wnt binding to its receptors inhibits glycogen synthase kinase 3 (GSK3), releasing β-catenin from the cytoplasmic degradation complex to free β-catenin. Excess β-catenin translocates to the nucleus and transcribes target genes such as cyclin D1, c-MYC, matrix metalloproteinase (MMP)-3 and CD44 (Baron and Kneissel, 2013; Corr, 2008).

The Wnt/ β-catenin signaling pathway promotes synovial hyperplasia, inflammation and pannus formation during the RA progression (Sen, 2005). It is related to the articular cartilage degradation in osteoarthritis, and increased levels of β-catenin were found in the articular

* Corresponding author at: Department of Morphology, Faculty of Medicine, Federal University of Ceará, Rua Delmiro de Farias, S/N, Rodolfo Teófilo, CEP: 60430-170 Fortaleza, CE, Brazil.
E-mail addresses: marianavale@ufc.br (M.L. Vale), delane@ufc.br (D.V. Gondim).

https://doi.org/10.1016/j.bonr.2022.101649
Received 20 October 2022; Received in revised form 27 November 2022; Accepted 16 December 2022
Available online 16 January 2023

chondrocytes, causing hypertrophy and matrix mineralization (Corr, 2008).

It is also known that this signaling pathway shows an essential role in the neuronal development, activating intracellular processes, such as: neurogenesis, neuroplasticity, axonal and dendritic branching and synapse formation (Shi et al., 2012). Furthermore, Wnt/ β-catenin pathway has been related to the pathogenesis of several types of pain, such as pain induced by peripheral nerve injury, chronic pain associated with multiple sclerosis, chronic pain associated with HIV, bone cancer pain, and diabetic neuropathy (Tang et al., 2022).

The TMJ inflammatory pain on rheumatic arthritis is conducted through the trigeminal pathway, and a previous study of our group showed that the Wnt/ β-catenin signaling pathway is increased in the TMJ of the arthritic rats (de Sousa et al., 2019). However, to the best of our knowledge, there are no studies relating its participation in the nociceptive trigeminal pathway. We believe that this investigation is necessary for the RA pathophysiological understanding in the TMJ, as well as, for exploring new therapies for the arthritic pain treatment. In this way, our study investigated the involvement of the Wnt/β-catenin on the articular cartilage injury and nociception of the TMJ experimental chronic arthritis.

2. Material and methods

2.1. Animals

The experimental protocols were approved by the Institutional Animal Use Ethics Committee of Federal University of Ceará (nº 4747280219), and followed the National Institutes of Health Guide for the Care and Use of Laboratory Animals (NIH Publications n. 8023, revised 1978) and the ARRIVE Guidelines UK. The sample size was determined from the study by de Sousa et al. (2019), to obtain a sample with 80 % power and 95 % confidence, adding two animals to each group considering possible losses. Thirty-two male Wistar rats (7–8 weeks old; 180–220 g; 3 animals/cage) were provided by the Central Animal Facility, Federal University of Ceará, and were kept in controlled temperature, 12 h/12 h light/dark cycle and easy access to water and food.

The animals were divided in two experimental protocols. In the first protocol, the animals of the experimental groups (n = 8 animals/group) were submitted to the evaluation of the mechanical hyperalgesia in the TMJ region and microscopic analysis of the TMJ articular cartilage. In the second protocol, it was performed the analysis of the c-Fos, Wnt10b and β-catenin immunoexpression in the trigeminal nociceptive pathway.

2.2. Induction of TMJ arthritis

Sixteen animals were randomized, using a computer based random order generator, into two groups: Control (C) and Rheumatoid Arthritis (RA). Both were initially sensitized with a subcutaneous injection containing 100 μl of phosphate buffered saline (PBS), 100 μl of complete Freund Adjuvant (CFA) and 500 μg of methylated bovine serum albumin (mBSA). Booster injections of mBSA dissolved in incomplete Freund Adjuvant (IFA) were given 7 and 14 days after the first immunization at different sites on the animal's back. Twenty-one days after the first injection, the arthritis was induced in the RA group with intra-articular injection of mBSA (10 μg/joint) dissolved in 10 μl PBS in the left TMJ. Booster injections in this joint were given on days 28 and 35. Animals were euthanized 24 h after the third injection (de Sousa et al., 2019). The C group received 0.9 % saline solution in the left TMJ (10 μl/joint) on days 21, 28 and 35.

2.3. Mechanical hyperalgesia

The animal's nociceptive threshold was obtained by recording the intensity of force applied in the TMJ region, necessary to obtain a reflex response (head withdrawal movement). For this, the electronic Von Frey device (Digital Analgesimeter, Insight, São Paulo, Brazil) was perpendicularly applied in the evaluated region. The animals were submitted to conditioning sessions to the mechanical hypernociception test five days before the subcutaneous induction. The animals were kept for 20 min in plastic boxes and submitted to application of the Von Frey device in the left TMJ region. The measurements were performed by a blind calibrated examiner. Tests were performed on days 0, 1, 7 and 14 after subcutaneous induction of mBSA and Freund's Adjuvant, and on days 20, 21, 28 and 35 after each intra-articular injection of mBSA or saline (de Sousa et al., 2019).

2.4. Histopathological analysis

The rats were euthanized, and the TMJs were fixed in 10 % buffered formalin solution and demineralized in 10 % EDTA solution. The tissues were embedded with paraffin and sections (4 μm) included the condyle, articular cartilage, articular disc, membrane and periarticular tissue. They were examined using light microscopy (Leica microscope). The specimens were stained with hematoxylin-eosin (HE) and Toluidine Blue. A qualitative description of the articular cartilage was made and the intensity of metachromasia was evaluated by an experienced pathologist, blinded to the groups. Areas of articular cartilage with greater intensity of violet staining indicate a higher concentration of proteoglycans (Costa et al., 2021; Lemos et al., 2016).

2.5. Collagen birefringence analysis

The left TMJs were incubated in picrosirius red (ScyTek®) for 30 min, and washed in 5 % hydrochloric acid, stained with Harris' hematoxylin and mounted with Enhtellan®. The slides were analyzed using a polarized light microscope (Leica - DM 2000), where collagen type I was performed with a red-orange color, and collagen type III with a white-green color. To quantify types I and III collagen, five fields at 400× magnification were photographed using a camera attached to the Leica DM 2000 Microscope. The photomicrographs were evaluated using ImageJ image analysis software (Ferreira et al., 2020).

2.6. Immunohistochemistry for TNF-a, IL-1β, IL-6, Wnt10b, β-catenin, c-Myc and cyclin D1

Immunohistochemistry for TNF-α, IL-1β, IL-6, Wnt10b, β-catenin, c-Myc and Cyclin D1 was performed by the streptavidin-biotin-peroxidase method in paraffin sections. The sections (4 μm thick) were deparaffinized, and after antigen recovery, with citrate buffer at 95 °C, endogenous peroxidase was blocked with 3 % (*v*/v) hydrogen peroxide for thirty minutes.

Sections were incubated with TNF-α (1:100; Abcam, Cambridge, UK), IL-1β (1:100; Abcam, Cambridge, UK), IL-6 (1:100; Santa Cruz Biotechnology, California, USA), Wnt10b (1:400; Abcam;), β-Catenin (1:200 dilution; DAKO; California, USA), c-Myc (1:200 dilution; Abcam, Cambridge, UK); Cyclin D1 (1:200; Abcam, Cambridge, UK); diluted in DAKO antibody thinner overnight. The sections were then incubated for 30 min with polymer (Invision Flex HRP, DAKO, California, USA). Only IL-6 was incubated with ABC complex (30 min), an avidin-peroxidase conjugate (Strep ABC complex, Santa Cruz Biotechnology, California, USA).

Antibody binding sites were visualized by incubation with diaminobenzidine-H_2O_2 solution (DAB, DAKO, California, USA). The sample sections that were incubated with antibody diluent, without primary antibody included, were considered negative controls. Positive staining for these antibodies was determined by brown staining at the level of cytoplasm in articular cartilage and synovial membrane. Immunolabeled cells were counted in five randomly selected fields (400×) under a microscope (Leica DM 2000, Wetzlar, Germany) (Costa et al., 2021).

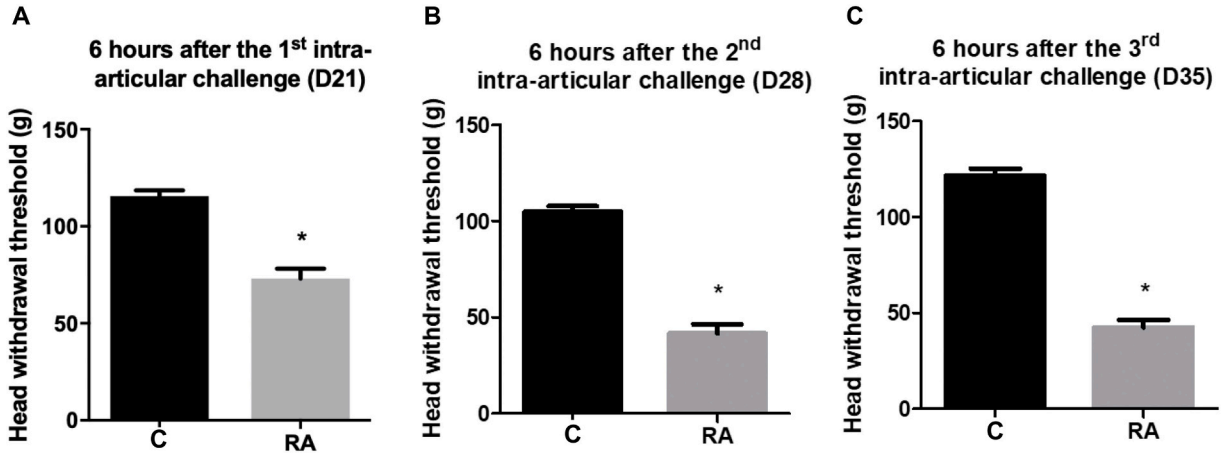

Fig. 1. Intra-articular injection of mBSA in the left TMJ reduces the nociceptive threshold. A. Mechanical hyperalgesia evaluation on the 6th hour after the first intra-articular challenge. B. A. Mechanical hyperalgesia evaluation on the 6th hour after the second intra-articular challenge. C. A. Mechanical hyperalgesia evaluation on the 6th hour after the third intra-articular challenge. Bars represent the mean ± SEM (n = 8); Student's *t*-test, * $p < 0.0001$; C = Control animals, RA = animals with RA in TMJ.

2.7. Immunofluorescence analysis for c-Fos, Wnt10b and β-catenin

Sixteen other animals were randomized in C and RA groups (n = 8/group) and the trigeminal ganglion and the caudal subnucleus of the trigeminal spinal tract (Sp5C) were removed. The trigeminal ganglion was removed and the three branches of the trigeminal nerve were kept. The Sp5C region was localized and the sections were cut-14 mm to −15 mm from the bregma (Paxinos and Watson, 1998). The dissected structures were placed in 4 % PFA for 2 h and cryoprotected in 30 % sucrose solution for 48 h. After this period, tissues were embedded in Tissue-tek and stored at −80 °C. For immunofluorescence assays, sections (10 μm) were fixed in methanol and antigen retrieval performed in 0.1 M (pH 6.0) of citrate buffer. Then, permeabilization of the nuclear membrane was performed with 0.1 % triton X-100. Non-specific sites were blocked with 5 % bovine serum albumin and 0.3 M glycine. The samples were incubated overnight with primary antibody anti-c-Fos (1:200, Cell Signaling Technology, Denvers, MA, USA) anti-Wnt10b (1:300; Abcam, Cambridge, UK) and anti-β-Catenin (1:300; Abcam, Cambridge, UK). Afterward, the incubation was carried out with rabbit anti-IgG antibody associated with Alexa fluor 568. To label the neuronal bodies, the samples were incubated with NeuN antibody conjugated with Alexa fluor 488. DAPI was added to show cell nuclei. For β-catenin analysis, the samples were also incubated with glutamine synthetase to highlight satellite cells.

Quantification of the fluorescent area in the photomicrographs, using confocal microscopy (Zeiss LSM 710, Carl Zeiss, Jena, Germany) was performed by differentiating the fluorescent pixels by the highest color saturation associated with fluorescence (red or green) with image analysis software (Fiji ImageJ, National Institutes of Health, Washington, DC, USA). Quantitation results were presented in percentage,

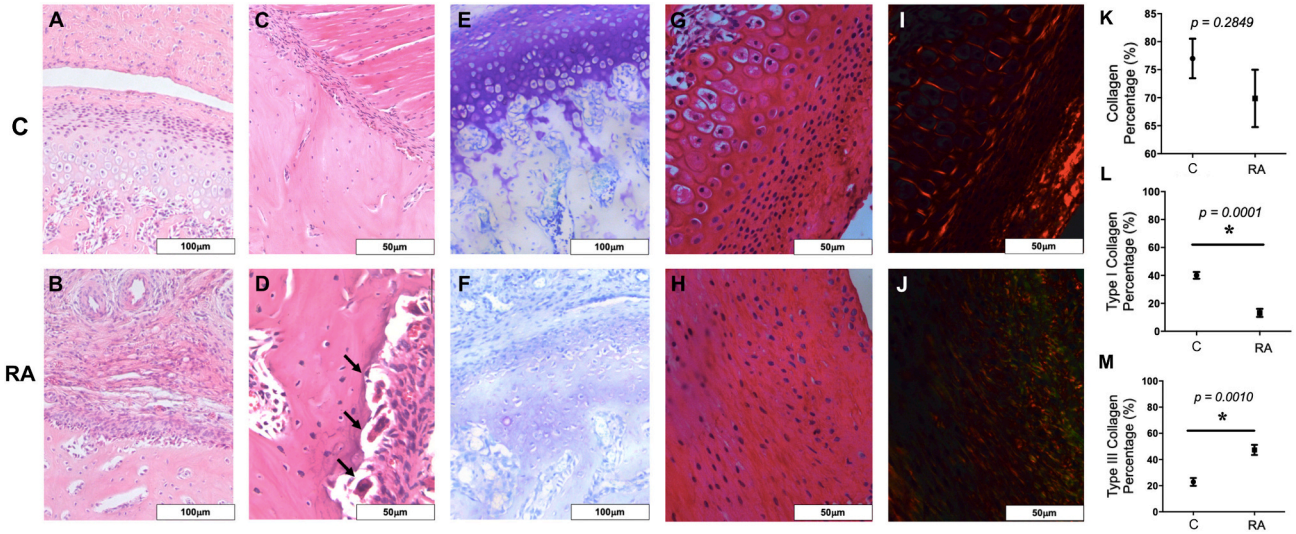

Fig. 2. A. Photomicrograph of the normal TMJ. HE staining. B. Photomicrograph of the arthritic TMJ, showing the articular damage. HE staining. C. Photomicrograph of the normal TMJ, highlighting the integrity of the bone covering layer. HE staining. D. Photomicrograph of the arthritic TMJ. Resorption of the bone covering layer and presence of osteoclasts. HE staining. E. Photomicrograph of the normal TMJ articular cartilage, showing intense metachromasia. Toluidine blue staining. F. Photomicrograph of the arthritic TMJ articular cartilage, showing reduction of the metachromasia. G. Photomicrograph of the normal TMJ articular cartilage. Picrosirius red staining. H. Photomicrograph of the arthritic TMJ articular cartilage. Picrosirius red staining. I. Photomicrograph of the normal TMJ stained with Picrosirius and analyzed in polarization microscopy. J. Photomicrograph of the arthritic TMJ stained with Picrosirius and analyzed in polarization microscopy, $^{x}40$ and $^{x}200$ magnification K. Collagen total percentage graph. Student's *t*-test; $p = 0.2849$. M. Type I collagen percentage graph. Student's t-test; $p < 0.0001$. N. Type III collagen percentage graph. Student's *t*-test; $p = 0.001$ Values are means ± SEM (n = 8); C = Control animals, RA = animals with RA in TMJ.

calculated by positive fluorescence in relation to NeuN fluorescence, and for β-catenin, in relation to Glutamine Synthetase fluorescence (Pontes et al., 2019). The image capture and the quantification were conducted by 2 independent and trained observers and blinded to the experimental conditions.

2.8. Statistical analysis

The Student's *t*-test was used to compare the mean between two groups of parametric data. Statistical analyzes were performed using SPSS 20.0 and GraphPad Prism 7 software (GraphPad Prism software, La Jolla, CA, USA). *P* values <0.05 were considered statistically significant.

3. Results

3.1. TMJ arthritis induced by mBSA causes mechanical hyperalgesia

The mechanical hyperalgesia evaluation in the left TMJ was performed on day 0 (immediately before the subcutaneous injection of mBSA and CFA) and on days 1, 7 and 14 (six hours after the subcutaneous inductions). No significant differences were observed between the groups, suggesting that the subcutaneous administration of mBSA did not induce alterations in the nociceptive threshold in the left TMJ.

Six hours after the first intra-articular injection of mBSA (21st day) in the left TMJ, a new recording was performed, and there was a significant reduction of the nociceptive threshold ($p = 0.0001$). On days 28 and 35, 6 h after the second and third intra-articular injection, respectively, the nociceptive threshold remained low, being statistically different in relation to the C group (p = 0.0001) (Fig. 1).

3.2. Histopathological analysis of the TMJ articular cartilage

In the histopathological analysis of the TMJ, no changes were observed in the articular cartilage in the C group (Fig. 2A). In the RA group, extensive destruction of the articular cartilage layers was observed, with the presence of a predominant mononuclear inflammatory infiltrate, with invasion of the pannus in the inferior joint cavity (Fig. 2B). In the C group, the bone covering layer remained intact (Fig. 2C). However, the RA group presented areas of articular destruction, containing sites of contact of osteoclasts with the bone matrix, forming depressions called Howship gaps (Fig. 2D).

The blue toluidine staining in the left TMJ showed an increased metachromasia in the articular cartilage in the C group. This suggests a high concentration of proteoglycans in the extracellular matrix (Fig. 2E). We observed an intense reduction of the metachromasia, a disorganization of the articular cartilage layers, suggesting articular cartilage damage and, consequently, a lower concentration of proteoglycans (Fig. 2F).

3.3. Analysis of the collagen birefringence in the TMJ articular cartilage

The C group showed an intense red-orange glow, indicating a higher degree of compaction and organization of type I collagen fibers when compared to the RA group (Fig. 2G, I). In arthritic animals, there was a significant reduction in red-orange fibers (collagen type I), in addition to a greater disorganization of the collagen fiber network and a higher intensity of greenish-white coloration (collagen type III), suggesting the presence of immature collagen (Fig. 2H, J).

The collagen quantification in the articular cartilage showed that it was filled by collagen in the C and RA groups, representing 77.00 ± 3.53 % and 69.86 ± 5.13 %, respectively ($p = 0.2849$) (Fig. 2K). The C group showed a significant increase ($p = 0.0001$) of area filled with collagen type I (40.06 ± 2.40 %) when compared to the RA group (13,24 ± 2,90 %) (Fig. 2L). However, the collagen type III percentage was significantly greater ($p = 0.001$) in the RA group (47,32 ± 3,58 %) when compared to C (22,88 ± 2,98 %).

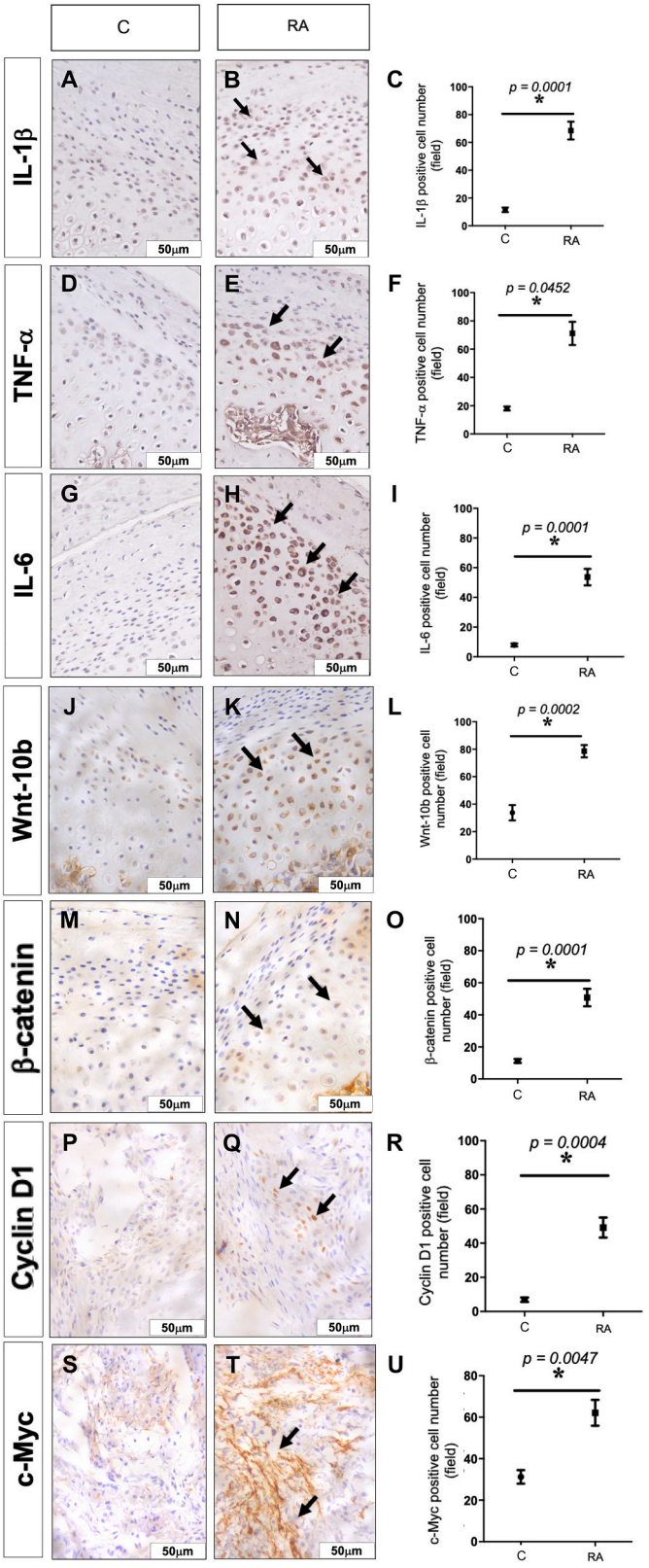

Fig. 3. Photomicrographs and increased immunoexpression of the IL-1®, TNF-<, IL-6, Wnt-10b, β-Catenin and Cyclin D1 in the articular cartilage and c-Myc in the TMJ synovial membrane. A–C IL-1®. D–F TNF-<. G-I IL-6. J-L Wnt-10b. M–O. β-Catenin P–R Cyclin D1. S–U c-Myc. ×400 magnification. Graphs represent the mean ± SEM (n = 8). Student *t*-test; C = Control animals, RA = animals with RA in TMJ.

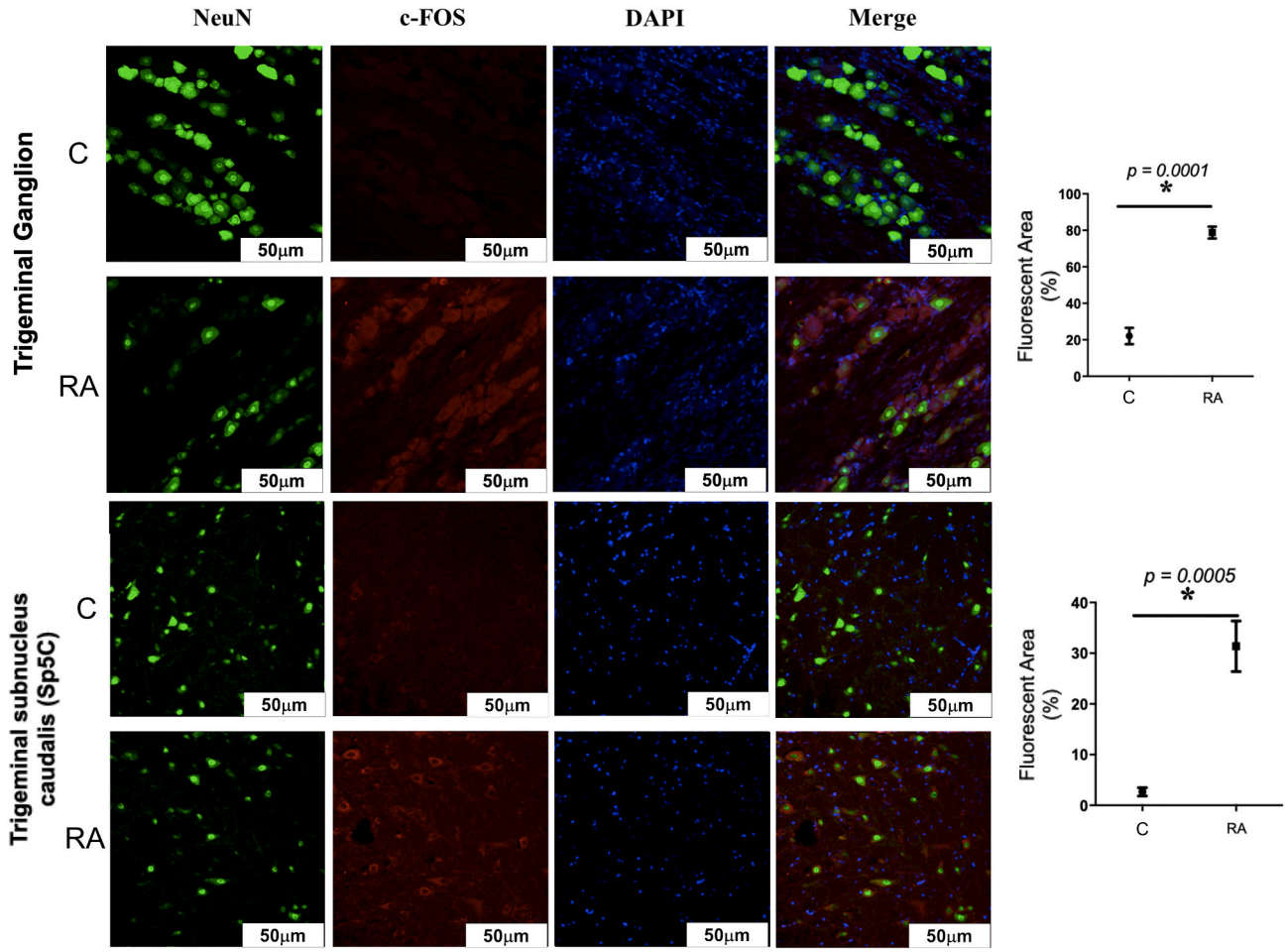

Fig. 4. Increased c-Fos expression in the trigeminal via in rats' TMJ arthritis A. c-Fos expression in trigeminal ganglion of rats submitted to rheumatoid arthritis induced by m-BSA. B. c-Fos expression in Sp5C of rats submitted to rheumatoid arthritis induced by m-BSA. Red: c-Fos; green: NeuN (neuronal marker); blue: DAPI (nuclear marker). C. Quantification of the fluorescent area of the c-Fos expression in trigeminal ganglion of rats submitted to rheumatoid arthritis induced by m-BSA. Student *t*-test; $p = 0.0001$. D. Quantification of the fluorescent area of the c-Fos expression in Sp5C region of rats submitted to rheumatoid arthritis induced by m-BSA The graphs represent the percentage of the positive fluorescent area in relation to NeuN. Student *t*-test; $p = 0.0005$. The data are expressed as the mean ± SEM (n = 8). C = Control animals, RA = animals with RA in TMJ.

3.4. Analysis of the immunoexpression for IL-1β, TNF-α, IL-6, Wnt10b, β-Catenin, Cyclin D1 in articular cartilage and c-Myc in synovial membrane

There was a significant increase of IL-1β, TNF-α, IL-6 ($p = 0.001$, respectively), Wnt10b ($p = 0.0002$), β-Catenin ($p = 0.0001$) and Cyclin D1($p = 0.0004$) in the articular cartilage in the arthritic rats. No c-Myc immunostaining was observed in the articular cartilage. A significant c-Myc expression was only found in the TMJ synovial membrane in the RA group ($p = 0.004$) (Fig. 3).

3.5. c-FOS, Wnt-10b and β-catenin immunoexpression in the nociceptive trigeminal pathway

There was a significant c-Fos staining in the trigeminal ganglion ($p = 0.0001$) and Sp5C region ($p = 0.0005$) in arthritic rats ($p = 0.0005$) (Fig. 4).

In the trigeminal ganglion, there was a significant Wnt10b immunostaining in the neuronal cells ($p = 0.0001$), while β-catenin had a significant increase in the satellite cells ($p = 0.0005$) (Fig. 5). No Wnt10b and β-catenin immunostaining were observed in the Sp5C region.

4. Discussion

The TMJ RA induction by intra-articular booster injection of mBSA reproduces the findings of a human RA and it activates the canonical Wnt signaling pathway, producing the increase of the inflammatory cytokines in the synovial membrane and nociceptive behavior (de Sousa et al., 2019). Our study revealed that this pathway also participates in the articular cartilage injury and that there is increased immunoexpression of Wnt10b and β-catenin in the trigeminal ganglion. It is important to highlight, to the best of our knowledge, that this is the first study that shows the involvement of the Wnt/β-catenin pathway in the nociceptive trigeminal pathway.

In the progression of the RA, inflammatory cells from the pannus migrate to the articular cartilage region, leading to the tissue degradation (McInnes and Schett, 2011). In this study, an increase in the immunoexpression of the IL-1β, TNF-α and IL-6 was observed in the articular cartilage of the arthritic rats and these cytokines may contribute to the articular destruction through the matrix metalloproteinases (MMPs) release and inhibition of the proteoglycan synthesis, suppressing the synthesis of type II and IX collagen, leading to an inadequate tissue repair (Ghassemi-Nejad et al., 2011; Narazaki et al., 2017).

The proteoglycan depletion and the collagen degradation lead to articular cartilage destruction, and the MMPs play a key role,

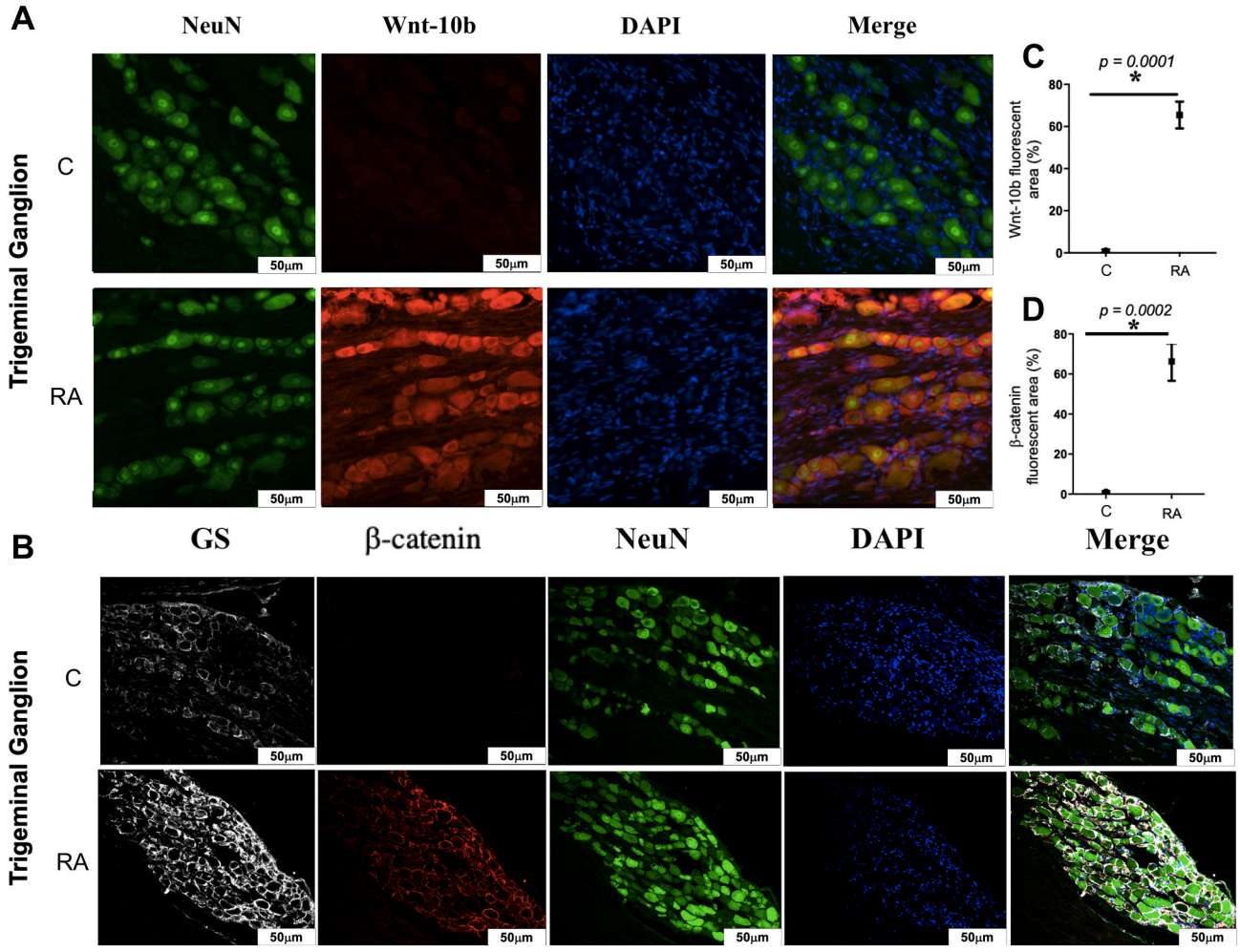

Fig. 5. Increased immunoexpression of Wnt-10b and β-Catenin in trigeminal ganglion of TMJ arthritic rats. A. Wnt-10b expression in trigeminal ganglion of rats submitted to rheumatoid arthritis induced by m-BSA. B β-Catenin expression in trigeminal ganglion of rats submitted to rheumatoid arthritis induced by m-BSA. Green: NeuN (neuronal marker); red: Wnt-10b or β-Catenin; blue: DAPI (nuclear marker) C. Quantification of the fluorescent area of the Wnt-10b expression in trigeminal ganglion of rats submitted to rheumatoid arthritis induced by m-BSA. Student *t*-test; $p = 0.0001$. D. Quantification of the fluorescent area of the β-Catenin expression in trigeminal ganglion of rats submitted to rheumatoid arthritis induced by m-BSA. Student t-test; $p = 0.0002$. The graphs represent the percentage of the positive fluorescent area in relation to NeuN. The data are expressed as the mean ± SEM (n = 8). C = Control group; RA = Arthritic group; GS = glutamine synthetase.

stimulating, for example, type I collagen degradation (Kuchler-Bopp et al., 2020). In an experimental model of chronic arthritis in the TMJ, the authors showed a lower intensity of red-orange coloration in the collagen birefringence, suggesting a breakdown of the collagen network, such as a destruction of the extracellular matrix components (Lemos et al., 2016). Salo and Raustia (1995) observed a greater amount of type III collagen in the mandibular condyle from a patient with RA, suggesting an attempt to repair the articular cartilage damage. In our study, we found a reduction in type I collagen and an increase in type III collagen in the rats' TMJ RA. These facts suggest that the measure of the collagen type in the articular cartilage may be useful in the arthritis diagnosis.

This study showed that both Wnt10b and β-catenin had a significant immunoexpression in the rats' TMJ RA. The canonical Wnt pathway is involved in the regulation of articular cartilage homeostasis, playing a crucial role in the cell proliferation and regulation of the chondrocyte phenotype (Zheng et al., 2017). A study in chondrocytes of the osteoarthritis patients showed that β-catenin and MMP- 13 promote the matrix degradation and occurrence of osteoarthritis (Zhang et al., 2018). Hua et al. (2022) showed that the intra-articular injection of a Wnt pathway inhibitor, SM04690, upregulates Wnt16 expression and reduces disease progression in TMJ osteoarthritis.

C-Myc and cyclin D1 are proteins which are also activated by the nuclear translocation of β-catenin. C-Myc is involved in cell activation, proliferation and transformation, being an important marker in the regulation of synovial cell growth (Lee et al., 2020). Studies have reported that the c-Myc suppression was able to effectively reduce synovial cell proliferation, inflammation, and the expression of cytokines such as TNF-α, showing the importance of this protein as a possible and important therapeutic target for RA (Hashiramoto et al., 1999; Lee et al., 2020). Cyclin D1 acts on the proliferation of chondrocytes, being a key protein in the cell cycle (Zheng et al., 2017). Sun et al. (2015) showed that the increased expression of cyclin D1 activated the Wnt/β-catenin pathway, stimulating chondrocyte cell apoptosis, and consequently, increasing the secretion of TNF-α, IL-1β and IL-6. The increase in the immunoexpression of these two markers is associated with the activation of the canonical Wnt pathway in the RA group.

The increased expression of pro-inflammatory cytokines in the RA causes articular cartilage injury, and also contributes to the establishment of peripheral painful sensitization. TNF-α and IL-1β act on primary sensory neurons, reducing their excitability threshold, thus contributing to hyperalgesia in RA (Bas et al., 2016). IL-6 can stimulate the release of the calcitonin gene-related peptide (CGRP), enhancing the activity in spinal neurons, therefore suggesting its direct action on nociceptive

neurons (Favalli, 2020). Brenn et al. (2007) showed that injections of IL-6 into the male rats' knee joints triggered increased responses of spinal neurons to mechanical stimulation, sensitizing C fibers.

Studies have shown that females develop higher levels of inflammation than males, due to the production of a higher proinflammatory immune response (Pinheiro et al., 2011; Strickland et al., 2012). In this way, males may show a lower pain response, affecting the initiation and maintenance of inflammatory and neuropathic pain. In our study, the nociceptive behavior was evaluated through the nociceptive threshold in the TMJ region and c-Fos expression, a neuronal activity marker, and its expression represents the activation of the nociceptive pathway. An increased c-Fos expression was observed in the trigeminal ganglion, that contains the cell body of the peripheral neuron, and in the Sp5C region, site of the first nociceptive synapsis of the trigeminal pathway.

In the sensory ganglia, neuron cell bodies are surrounded by satellite cells, and the neuron-satellite cell communication has been implicated in the pain chronicity and inflammatory processes (Takeda et al., 2007). After peripheral injury, the satellite cells react by exhibiting morpho-physiological alterations secondary to neuronal alterations, implying the activation of signaling mechanisms between neurons and these cells. Takeda et al. (2007) showed that satellite cells can modulate the excitability of the trigeminal ganglion nociceptive neurons via IL-1β, inducing depolarization and increased expression of interleukin-1 receptor (IL-1R) in the neuronal body.

In our study, an increased expression of Wnt10b and β-catenin was observed in neurons and satellite cells in the trigeminal ganglion, respectively. Kim et al. (2021) showed in a model of paclitaxel-induced neuropathic pain that there is increased expression of Wnt3a, Wnt10a and calcitonin gene-related peptide (CGRP) in the spinal cord dorsal root ganglion and β -catenin in satellite cells. In this study, the authors showed that the administration of an antagonist of the canonical Wnt pathway reduced the expression of TNF-α, IL-1β, monocyte chemotactic protein-1 (MCP-1), Wnt3a, and Wnt10a.

Canonical Wnt signaling pathway contributes to neuronal sensitization in pathological disorders. The activation of the signaling pathway causes an increased production of proinflammatory cytokines and regulates the NR2B glutamate receptor and Ca^{+2} dependent signals through the β-catenin in the spinal cord (Zhang et al., 2013). Studies have shown that Wnt3a and β-catenin proteins are expressed in spinal cord ganglion and dorsal horn and that the Wnt/β-catenin signaling pathway induces neuropathic pain through brain-derived neurotrophic factor (BDNF) releasing from spinal microglial (Zhang et al., 2013; Zhou et al., 2020).

In our study, an increased expression of Wnt10b and β-catenin was observed only in the trigeminal ganglion and an increase in c-Fos expression along the nociceptive trigeminal pathway. There was no immunoexpression of Wnt10b and β-catenin in the trigeminal spinal tract at the evaluated time of 24 h after the third intra-articular injection of mBSA (Supplemental File). Our results suggest that the canonical Wnt pathway can be involved in the peripheral sensitization in this experimental model. Thus, we believe that to better understanding the participation of the canonical Wnt pathway, further studies should be carried out to evaluate the kinetics of immunoexpression of these proteins along the nociceptive trigeminal pathway at different times after the induction of TMJ RA, as well as to investigate the therapeutic potential of intra-articular injection of signaling pathway inhibitors in the TMJ inflammation and maintenance of the pain in the RA.

5. Conclusions

The RA in the rats' TMJ causes mechanical hyperalgesia and increases inflammatory parameters, followed by increased immunoexpression of Wnt10b and β-catenin in the articular cartilage and trigeminal ganglion.

Supplementary data to this article can be found online at https://doi.org/10.1016/j.bonr.2022.101649.

Funding

This research received no grant from any funding agency, commercial or not-for-profit sectors.

CRediT authorship contribution statement

L.M.S. and A.C.F·C: conception, data acquisition and interpretation, drafted and critically reviewed the manuscript. A.F.P., C.S.M. and O.V. O·F: data acquisition and interpretation. P.G. and M.L.V.: conception, design, data acquisition and interpretation. D.V.G.: conception, design, coordinated the experiments, drafted and critically reviewed the manuscript.

Declaration of competing interest

The authors declare no potential conflicts of interest with respect to the authorship and/or publication of this article.

Data availability

Data will be made available on request.

Acknowledgments

The authors gratefully acknowledge the Nucleus of Studies in Microscopy and Imaging Processing (NEMPI) the Center for Research and Drug Development (NPDM) of Federal University of Ceará and the Central Analítica-UFC/CT-INFRA/MCTI-SISANO/Pró-Equipamentos CAPES for their support.

References

Ahmed, U., Anwar, A., Savage, S.S., Costa, M.L., Mackay, N., Filer, A., et al., 2015. Biomarkers of early stage osteoarthritis, rheumatoid arthritis and musculoskeletal health. Sci. Rep. 5, 9259. https://doi.org/10.1038/srep09259.

Baron, R., Kneissel, M., 2013. WNT signaling in bone homeostasis and disease: from human mutations to treatments. Nat. Med. 19, 179–192. https://doi.org/10.1038/nm.3074.

Bas, D.B., Su, J., Wigerblad, G., Svensson, C., 2016. Pain in rheumatoid arthritis: models and mechanisms. Pain Manag. 6 (3), 265–284. https://doi.org/10.2217/pmt.16.4.

Brenn, D., Richter, F., Schaible, H.-G., 2007. Sensitization of unmyelinated sensory Wbres of the joint nerve to mechanical stimuli by interleukin-6 in the rat. An inXammatory mechanism of joint pain. Arthritis Rheum. 56, 351–359. https://doi.org/10.1002/art.22282.

Corr, M., 2008. Wnt–β-catenin signaling in the pathogenesis of osteoarthritis. Nat. Clin. Pract. Rheumatol. 4 (10), 550–556. https://doi.org/10.1038/ncprheum0904.

Costa, A.C.F., de Sousa, L.M., Alves, J.M.A., Goes, P., Pereira, K.M.A., Alves, A.P.N.N., et al., 2021. Anti-inflammatory and hepatoprotective effects of quercetin in an experimental model of rheumatoid arthritis. Inflammation 44 (5), 2033–2043. https://doi.org/10.1007/s10753-021-01479-y.

Covert, L., Mater, H.V., Hechler, B.L., 2021. Comprehensive management of rheumatic diseases affecting the temporomandibular joint. Diagnostics 11 (3), 409. https://doi.org/10.3390/diagnostics11030409.

de Sousa, L.M., Alves, J.M.S., Martins, C.S., Pereira, K.M.A., Goes, P., Gondim, D.V., 2019. Immunoexpression of canonical Wnt and NF-κB signaling pathways in the temporomandibular joint of arthritic rats. Inflamm. Res. 68, 889–900. https://doi.org/10.1007/s00011-019-01274-4.

Favalli, E.G., 2020. Understanding the role of interleukin-6 (IL-6)in the joint and beyond: a comprehensive review of IL-6 inhibition for the management of rheumatoid arthritis. Rheumatol. Ther. 7 (3), 473–516. https://doi.org/10.1007/s40744-020-00219-2.

Ferreira, A.E.C., Barros-Silva, P.G., Oliveira, C.C.O., Verde, M.E.Q.L., Sousa, F.B., Mota, M.R.L., et al., 2020. Influence of infliximab therapy on bone healing post-dental extraction in rats. Arch. Oral Biol. 112, 104680 https://doi.org/10.1016/j.archoralbio.2020.104680.

Ghassemi-Nejad, S., Kobezda, T., Rauch, T.A., Matesz, C., Glant, T.T., Mikecz, K., 2011. Osteoarthritis-like damage of cartilage in the temporomandibular joints in mice with autoimmune inflammatory arthritis. Osteoarthr. Cartil. 19 (4), 458–465. https://doi.org/10.1016/j.joca.2011.01.012.

Hashiramoto, A., Sano, H., Maekawa, T., Kawahito, Y., Kimura, S., Kusaka, Y., et al., 1999. C-Myc antisense oligodeoxynucleotides can induce apoptosis and down-regulate Fas expression in rheumatoid synoviocytes. Arthritis Rheum. 42 (5), 954–962. https://doi.org/10.1002/1529-0131(199905)42:5<954::AID-ANR14>3.0.CO;2-J.

Hua, B., Qiu, J., Ye, X., Liu, X., 2022. Intra-articular injection of a novel Wnt pathway inhibitor, SM04690, upregulates Wnt16 expression and reduces disease progression in temporomandibular joint osteoarthritis. Bone 158, 116372. https://doi.org/10.1016/j.bone.2022.116372.

Humphries, A.C., Mlodzik, M., 2018. From instruction to output: Wnt/PCP signaling in development and cancer. Curr. Opin. Cell Biol. 51, 110–116. https://doi.org/10.1016/j.ceb.2017.12.005.

Kim, H.K., Bae, J., Lee, S.H., Bae, H.L., Hwang, S.H., Kim, M.S., et al., 2021. Blockers of Wnt3a, Wnt10a, or β-catenin prevent chemotherapy-induced neuropathic pain in vivo. Neurotherapeutics 18 (1), 601–614. https://doi.org/10.1007/s13311-020-00956-w.

Kroese, J.M., Volgenant, C.M.C., Schaardenburg, D.V., Loss, B.G., Crielaard, W., Lobbezoo, F., 2020. Temporomandibular joint function, periodontal health, and oral microbiome in early rheumatoid arthritis and at-risk individuals: a prospective cohort study protocol. BDJ Open 6, 7. https://doi.org/10.1038/s41405-020-0034-8.

Kuchler-Bopp, S., Mariotte, A., Strub, M., Po, C., de Cauwer, A., Schulz, G., et al., 2020. Temporomandibular joint damage in K/BxN arthritic mice. Int. J. Oral Sci. 12 (1), 5. https://doi.org/10.1038/s41368-019-0072-z.

Lee, Y., Guo, H., Zhao, G., Yang, C., Chang, H., Yan, R., et al., 2020. Tylophorine-based compounds are therapeutic in rheumatoid arthritis by targeting the caprin-1 ribonucleoprotein complex and inhibiting expression of associated c-Myc and HIF-1⟨. Pharmacol. Res. 152, 104581 https://doi.org/10.1016/j.phrs.2019.104581.

Lemos, G.A., Rissi, R., Pires, I.L.S., Oliveira, L.P., Aro, A.A., Pimentel, E.R., Paslomari, E. T., 2016. Low-level laser therapy stimulates tissue repair and reduces the extracellular matrix degradation in rats with induced arthritis in the temporomandibular joint. Lasers Med. Sci. 31 (6), 1051–1059. https://doi.org/10.1007/s10103-016-1946-3.

McInnes, I.B., Schett, G., 2011. The pathogenesis of rheumatoid arthritis. N. Engl. J. Med. 365 (23), 2205–2219. https://doi.org/10.1056/NEJMra1004965.

Mustafa, M.A., Al-Attas, B.A., Badr, F.F., Jadu, F.M., Wali, S.O., Bawazi, Y.M., 2022. Prevalence and severity of temporomandibular disorders in rheumatoid arthritis patients. Cureus 14 (1), e21276. https://doi.org/10.7759/cureus.21276.

Narazaki, M., Tanaka, T., Kishimoto, T., 2017. The role and therapeutic targeting of IL-6 in rheumatoid arthritis. Expert. Rev. Clin. Immunol. 13, 535–551. https://doi.org/10.1080/1744666x.2017.1295850.

Paxinos, G., Watson, C., 1998. The Rat Brain in StereotaxicCoordinates, 4th ed. Academic Press, San Diego.

Pinheiro, I., Dejager, L., Libert, C., 2011. X-chromosome-located microRNAs in immunity: might they explain male/female differences? The X chromosome-genomic context may affect X-located miRNAs and downstream signaling, thereby contributing to the enhanced immune response of females. Bioessays 33 (11), 791–802. https://doi.org/10.1002/bies.201100047.

Pontes, R.B., Lisboa, M.R.P., Pereira, A.F., Lino, J.A., Oliveira, F.B., Mesquita, A.K.V., et al., 2019. Involvement of endothelin receptors in peripheral sensory neuropathy induced by oxaliplatin in mice. Neurotox. Res. 36, 688–699. https://doi.org/10.1007/s12640-019-00074-2.

Ruparelia, P.B., Shah, D.S., Ruparelia, K., Sutaria, S.P., Pathak, D., 2014. Bilateral TMJ involvement in rheumatoid arthritis. Case Rep. Dent. 2014, 262430 https://doi.org/10.1155/2014/262430.

Salo, L.A., Raustia, A.M., 1995. Type II and type III collagen in mandibular condylar cartilage of patients with temporomandibular joint pathology. J. Oral Maxillofac. Surg. 53, 39–44. https://doi.org/10.1016/0278-2391(95)90498-0.

Sen, M., 2005. Wnt signalling in rheumatoid arthritis. Rheumatology 44, 708–713. https://doi.org/10.1093/rheumatology/keh553.

Shi, Y., Yuan, S., Li, B., Wang, J., Carlton, S.M., Chung, K., et al., 2012. Regulation of Wnt signaling by nociceptive input in animal models. Mol. Pain 8, 47. https://doi.org/10.1186/1744-8069-8-47.

Singh, V., Holla, S., Ramachandra, S.G., Balaji, K.N., 2015. WNT-inflammasome signaling mediates NOD2-induced development of acute arthritis in mice. J. Immunol. 194, 3351–3360. https://doi.org/10.4049/jimmunol.1402498.

Sodhi, A., Naik, S., Pai, A., Anuradha, A., 2015. Rheumatoid arthritis affecting temporomandibular joint. Contemp. Clin. Dent. 6 (1), 124–127. https://doi.org/10.4103/0976-237X.149308.

Strickland, F.M., Hewagama, A., Lu, Q., Wu, A., Hinderer, R., Webb, R., et al., 2012. Environmental exposure, estrogen, and two X chromosomes are required for disease development in an epigenetic model of lupus. J. Autoimm. 38 (2–3), J135–J143. https://doi.org/10.1016/j.jaut.2011.11.001.

Sun, J., Yan, P., Chen, Y., Chen, Y., Yang, J., Xu, G., et al., 2015. MicroRNA-26b inhibits cell proliferation and cytokine secretion in human RASF cells via the Wnt/GSK-3β/β-catenin pathway. Diagn. Pathol. 10, 72. https://doi.org/10.1186/s13000-015-0309-x.

Takeda, M., Tanimoto, T., Kadoi, J., Nasu, M., Takahashi, M., Kitagawa, J., Matsumoto, S., 2007. Enhanced excitability of nociceptive trigeminal ganglion neurons by satellite glial cytokine following peripheral inflammation. Pain 129 (1–2), 155–166. https://doi.org/10.1016/j.pain.2006.10.007.

Tang, Y., Chen, Y., Liu, R., Li, W., Hua, B., Bao, Y., 2022. Wnt signaling pathways: a role in pain processing. Neuromol.Med. 24 (3), 233–249. https://doi.org/10.1007/s12017-021-08700-z.

van den Bosch, M.H., Blom, A.B., Kram, V., Maeda, A., Sikka, S., Gabet, Y., et al., 2017. WISP1/CCN4 aggravates cartilage degeneration in experimental osteoarthritis. Osteoarthr. Cartil. 25, 1900–1911. https://doi.org/10.1016/j.joca.2017.07.012.

Zhang, Y.K., Huang, Z.J., Liu, S., Liu, Y.P., Song, A.A., Song, X.J., 2013. WNT signaling underlies the pathogenesis of neuropathic pain in rodents. J. Clin. Investig. 123 (5), 2268–2286. https://doi.org/10.1172/jci65364.

Zhang, H.X., Sun, C., Yu, H.C., Song, B., Pan, Z.X., 2018. Targeted inhibition of β-catenin by miR-320 and decreased MMP-13 expression in suppressing chondrocyte collagen degradation. Eur. Rev. Med. Pharmacol. Sci. 22 (18), 5828–5835. https://doi.org/10.26355/eurrev_201809_15909.

Zheng, W., Lin, P., Ma, Y., Shao, X., Chen, H., Chen, D., et al., 2017. Psoralen promotes the expression of cyclin D1 in chondrocytes via the Wnt/β-catenin signaling pathway. Int. J. Mol. Med. 40 (5), 1377–1384. https://doi.org/10.3892/ijmm.2017.3148.

Zhou, X., Tao, L., Zhao, M., Wu, S., Obeng, E., Wang, D., Zhang, W., 2020. Wnt/ β-catenin signaling regulates brain-dereived neurotrophic fator release from spinal micróglia to mediate HIV, gp120-induced neuropathic pain. Mol. Pain 16, 1–14. https://doi.org/10.1177/1744806920922100.